

Exposure to the Tire Rubber-Derived Contaminant 6PPD-Quinone Causes Mitochondrial Dysfunction *In Vitro*

Hannah Mahoney, Francisco C. da Silva Junior, Catherine Roberts, Matthew Schultz, Xiaowen Ji, Alper James Alcaraz, David Montgomery, Summer Selinger, Jonathan K. Challis, John P. Giesy, Lynn Weber, David Janz, Steve Wiseman, Markus Hecker, and Markus Brinkmann*



Cite This: <https://doi.org/10.1021/acs.estlett.2c00431>



Read Online

ACCESS |

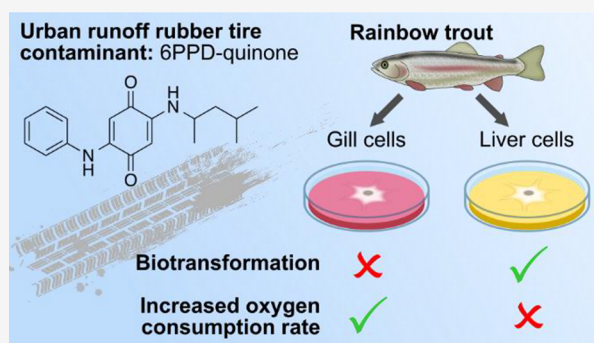
Metrics & More

Article Recommendations

Supporting Information

ABSTRACT: *N*-(1,3-Dimethylbutyl)-*N'*-phenyl-*p*-phenylenediamine-quinone (6PPD-quinone), a rubber tire oxidation product found in road runoff, is highly and acutely toxic to selected salmonids including coho salmon, brook trout, and rainbow trout but not other fish species and invertebrates studied to date. Sensitive species displayed increased ventilation and gasping, suggesting a possible impact on respiration. Here, adherent cell lines RTL-W1 and RTgill-W1 were exposed to 5–80 $\mu\text{g/L}$ 6PPD-quinone, and cytotoxicity, oxygen consumption rate (OCR), and biotransformation of 6PPD-quinone were measured to assess the ability of 6PPD-quinone to uncouple mitochondrial respiration *in vitro*. RTL-W1 cells were not sensitive to 6PPD-quinone, and exposure did not result in significant impacts on cytotoxicity or OCR. In contrast, RTgill-W1 cells demonstrated decreased cell viability at 80 $\mu\text{g/L}$ and a 2-fold increase in OCR at 20 $\mu\text{g/L}$. Effects appear to be partly driven by toxicokinetic differences where incubation of RTL-W1 cells with 6PPD-quinone led to almost quantitative conversion of 6PPD-quinone into a suspected hydroxy-metabolite, which was not observed in RTgill-W1 cells. Exposure studies with primary cultures of rainbow trout gill cells indicated that 6PPD-quinone increased OCR by uncoupling the mitochondrial electron transport chain. Together, these findings suggest that 6PPD-quinone toxicity might be driven by a tissue-specific disruption of mitochondrial respiration.

KEYWORDS: *N*-(1,3-dimethylbutyl)-*N'*-phenyl-*p*-phenylenediamine-quinone, *Oncorhynchus mykiss*, cell lines, *in vitro*, oxidative phosphorylation, uncoupler



INTRODUCTION

Recently, there have been alarming reports of mass die-off of salmon along the western coast of North America, from northern California, USA, to British Columbia, Canada.^{1,2} These events, referred to as urban runoff mortality syndrome (URMS), occurred near urban areas after heavy rains and were most frequently observed in Pacific Northwest coho salmon (*Oncorhynchus kisutch*).^{1–4} As a result, 40%–90% of adult coho salmon returning to spawn in freshwaters near urbanized watersheds can experience mortality, which threatens the conservation of the species.⁵ Recently, *N*-(1,3-dimethylbutyl)-*N'*-phenyl-*p*-phenylenediamine-quinone (6PPD-quinone) was identified as the primary toxicant responsible for URMS in coho salmon.⁶ 6PPD-quinone is formed in the environment through the oxidation of the antioxidant 6PPD, which is widely used in rubber tires and can accumulate on road surfaces before entering the aquatic environment in stormwater runoff.⁷ Once 6PPD-quinone was identified as the cause of URMS, efforts shifted toward identifying effects of 6PPD-quinone on other aquatic receptors to develop a species sensitivity distribution and to identify the mechanism underlying 6PPD-

quinone toxicity.^{6,8–11} Most interestingly, coho salmon, brook trout (*Salvelinus fontinalis*), and rainbow trout (*Oncorhynchus mykiss*) were exceptionally susceptible to acute lethality caused by exposure to 6PPD-quinone at concentrations ranging from 0.1 to 1.0 $\mu\text{g/L}$, while all other species tested, including zebrafish (*Danio rerio*), Japanese medaka (*Oryzias latipes*), Arctic char (*Salvelinus alpinus*), and white sturgeon (*Acipenser transmontanus*), as well as the invertebrates *Hyalella azteca*, *Brachionus calyciflorus*, and *Daphnia magna*, were highly tolerant.^{8–10,12}

Although 6PPD-quinone has been identified as the primary cause of URMS, the mechanism by which it causes its species-specific acute lethality is not known. Varshney et al.¹⁰ reported

Received: June 25, 2022

Revised: August 1, 2022

Accepted: August 2, 2022

an increased oxygen consumption rate (OCR) in zebrafish larvae exposed to 10 $\mu\text{g/L}$ 6PPD-quinone despite a decreased heart rate, which could be the result of hypoxic bradycardia, which is often observed as a result of exposure to toxicants that affect cardiorespiratory function.^{10,13,14} Strategies used by fish to increase oxygen uptake (gasping, increased ventilation rate) can be indicative of electron transport chain inhibition or uncoupling.^{15–17} This suggests that 6PPD-quinone might cause acute toxicity by disrupting respiration, but this hypothesis has yet to be explored. It is also currently unclear if toxicokinetic species differences, i.e., differences in their ability to detoxify or bioactivate 6PPD-quinone, could be significant drivers of toxicity.

The present study investigated whether 6PPD-quinone can disrupt mitochondrial function, which has been suggested as a potential mechanism of the acute lethality observed in selected fishes. This hypothesis was tested using *in vitro* OCR assays using adherent cultures of the immortalized rainbow trout liver and gill cells, RTL-W1 and RTgill-W1, respectively. A nontarget analytical workflow was applied to tentatively identify intermediate and biotransformation products of 6PPD-quinone generated in a biotransformation assay using these cell lines. On the basis of the results of these screening assays, effects of 6PPD-quinone on OCR were investigated in suspensions of primary rainbow trout gill cells.

MATERIALS AND METHODS

Chemicals. 6PPD-quinone and mass-labeled 6PPD-quinone- d_5 were purchased from Toronto Research Chemicals (Canada) and had purities of $\geq 97\%$. Stock solutions for exposure of cells were prepared in dimethyl sulfoxide (DMSO) to achieve a final solvent concentration of 0.1% (v/v) in cell media. Standard solutions of native and isotopically labeled 6PPD-quinone were prepared in HPLC-grade methanol.

Cell Culture. Two rainbow trout cell lines, RTL-W1 and RTgill-W1, were obtained from Dr. Lucy Lee (University of the Fraser Valley, Canada). Cells were grown in 75 cm^2 tissue culture flasks at 18°C in L-15 medium supplemented with 10% fetal bovine serum (FBS) and 1% penicillin–streptomycin (Fisher Scientific, Canada). Cells between passage numbers 50 and 70 were used in bioassays when they had reached 90% confluency.

Cytotoxicity Assay. Cytotoxicity was determined based on the mitochondria-dependent reduction of 3-(4,5-dimethylthiazol-2-yl) 2,5-diphenyl-tetrazolium bromide (MTT) (Sigma-Aldrich, Canada) to formazan and accumulation of neutral red dye (Sigma-Aldrich), following established protocols,^{18,19} with some modifications. Briefly, RTL-W1 and RTgill-W1 cells were plated at a density of 60,000 cells/well in 96-well plates for 24 h. After a subsequent 24 h of exposure to 6PPD-quinone at 5, 10, 20, 40, and 80 $\mu\text{g/L}$, cells were washed with PBS twice, followed by incubation with MTT (1 mg/mL) or neutral red (40 $\mu\text{g/mL}$) for 2 and 4 h, respectively. Cells were washed twice with PBS, and the dyes were extracted in either 100 μL of 100% DMSO (MTT) or 100 μL of destaining solution (50% ethanol, 49% deionized water, and 1% glacial acetic acid (v/v); neutral red). Absorbance was measured at 570 and 540 nm for MTT and neutral red assays, respectively (TECAN Life Sciences, Switzerland). Results were expressed as percent viability relative to the solvent control. Assays were repeated three times as independent assays, each with six replicate wells per treatment.

Oxygen Consumption Rate Assay. RTL-W1 and RTgill-W1 cells were seeded into 96-well plates at a density of 5000 cells/well in 200 μL ($\sim 1 \times 10^5$ cells/mL) and allowed to adhere for 24 h before the culture medium was replaced with media containing 5, 10, 20, 40, or 80 $\mu\text{g/L}$ of 6PPD-quinone in 0.1% DMSO. OCR was quantified using a commercial OCR Assay Kit according to the manufacturer's instructions (Cayman Chemicals, USA). OCR was measured by use of a phosphorescent probe that is quenched in the presence of oxygen, resulting in a signal that is inversely proportional to dissolved oxygen concentrations (Cayman). Briefly, cells were incubated with a phosphorescent oxygen probe and overlaid with mineral oil, and phosphorescence (excitation wavelength, 380 nm; emission wavelength, 650 nm) was read kinetically in 5 min intervals using a Spark multimode plate reader (TECAN). The initial OCR of cells exposed to 6PPD-quinone was expressed as x -fold changes relative to the solvent control (0.1% DMSO). Differences between treatments and controls were evaluated using one-way ANOVA with Dunnett's posthoc test. Assays were repeated three times as independent assays, each with six replicate wells per treatment.

Biotransformation Assay. These experiments followed the workflow outlined by Brinkmann et al.²⁰ RTL-W1 and RTgill-W1 cells were transferred to 25 cm^2 tissue culture flasks and grown to confluency. Culture media was replaced with 5 mL of L-15 media containing 5% FBS and penicillin–streptomycin (negative control, or media containing 20 $\mu\text{g/L}$ 6PPD-quinone). Cells were exposed for 24 h before the exposure media was aspirated and stored in 15 mL centrifuge tubes. Cells were detached using cell scrapers, precipitated, extracted using 5 mL of 4°C acetonitrile, and stored in 15 mL centrifuge tubes. Supernatant and cell samples were flash-frozen in nitrogen and stored at -80°C until analysis. Solvent control and treatment flasks were exposed in triplicate for both cell lines.

Analysis of 6PPD-quinone in supernatants and cells was conducted using a Vanquish ultrahigh performance liquid chromatography (UHPLC) system coupled with a Q-Exactive HF mass spectrometer (Thermo Fisher, Canada). The chromatographic separation was achieved using a Kinetex 1.7 μm XB-C18-LC column (100 $\text{mm} \times 2.1$ mm) (Phenomenex, Torrance, CA) and followed by gradient elution (details can be found in Challis et al.⁷), containing a polar solvent (95% water; 5% methanol; 0.1% formic acid) and an organic solvent (100% methanol; 0.1% formic acid), with a flow rate of 0.2 mL/min and column compartment temperature of 40 °C. Quantification of 6PPD-quinone followed previously published isotope-dilution methods using 6PPD-quinone- d_5 .^{6,7} Additionally, data-dependent MS2 (ddMS2) acquisition, where precursor ions were sequentially selected from full scans based on the intensity of parent ions, was used to screen for potential biotransformation products of 6PPD-quinone. The suspected metabolite was manually checked by comparison of chromatogram and corresponding MS2 mass spectra from the negative control and exposed samples (Figures S1–S5), where ion chromatograms are filtered with 5 ppm mass tolerance. Analytical standards for metabolites were unavailable; thus, concentrations were semiquantified assuming their response was equal to that of 6PPD-quinone.

Respirometry Experiments with Suspensions of Primary Gill Cells. Cellular respirometry was carried out using a temperature-controlled Oxytherm+R system (Hansa-

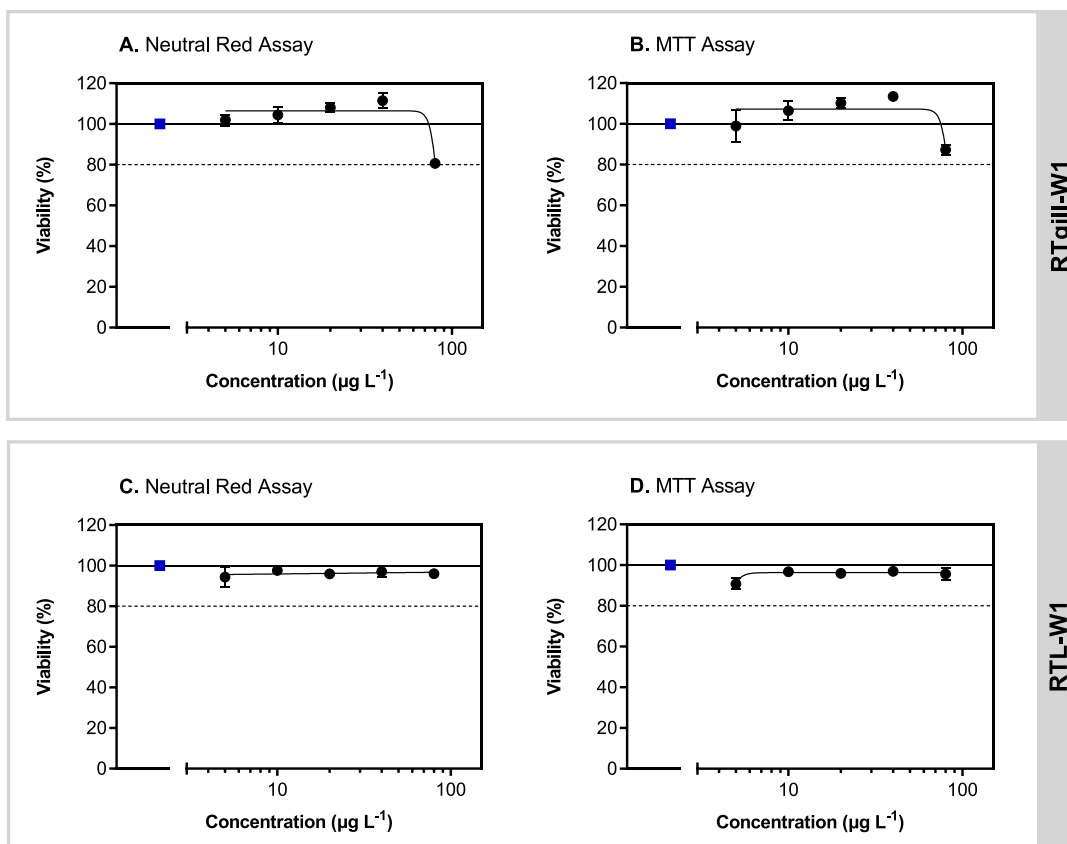


Figure 1. Viability of RTgill-W1 (A, B) and RTL-W1 (C, D) cells exposed to graded concentrations of 6PPD-quinone as determined using the neutral red retention (A, C) and MTT (B, D) assays. Viabilities of treated cells were expressed relative to that of the solvent control (blue squares). Symbols indicate the arithmetic mean and errors bars the standard deviations of $n = 3$ independent biological replicate plates.

tech, UK) at 20 °C, with an S1 Clark-type polarographic oxygen disc electrode²¹ and a magnetic stirrer at 900 rpm.

Assays were performed using primary gill cells from subadult rainbow trout (source, Lyndon Hatcheries, ON, Canada; weight, 277 ± 37 g; length, 28.6 ± 0.46 cm; 6–8 gill arches each). Permission for animal use was obtained from the University of Saskatchewan Animal Care Committee (protocol 20070049). Primary gill cells were prepared using modified versions of previously published protocols.^{22,23} Briefly, fish were euthanized in 250 mg/L buffered tricaine mesylate. Gill arches were excised and washed in Hanks' Balanced Salt Solution (HBSS, Gibco). Each arch was digested in a centrifuge tube with 2 mL of trypsin solution (Gibco) for 20 min at 12 °C. The arches were removed, and the digestion was stopped by adding 4 mL of mitochondrial respiration buffer (MRB), which contained 20 mM HEPES, 0.5 mM EGTA, 3 mM MgCl₂, 60 mM lactobionic acid, 20 mM taurine, 110 mM mannitol, 0.3 mM dithiothreitol, 10 mM KH₂PO₄, and 1 g/L bovine serum albumin dissolved in ultrapure water. Gill arches were placed in fresh trypsin for a second digestion, after which suspensions were combined and strained through a 70 µm cell strainer. The suspension was centrifuged for 10 min at 500g and 12 °C, the supernatant removed, and cells resuspended in 10 mL of MRB. Viability and density of cells were determined using a hemocytometer and Trypan blue exclusion. Cell density ranged from 11.5 to 39 million cells per mL, with viability consistently greater than 95%.

With this assay, changes in respiration in response to a known uncoupler, carbonyl cyanide *p*-trifluoromethoxyphenyl-

hydrazone (FCCP), were compared to that of 6PPD-quinone, a suspected uncoupler. Gill cells were introduced to the chamber and cofactor solutions (15 µL of 200 mM malate, 60 µL of 250 mM glutamate, 15 µL of 500 mM pyruvate, and 30 µL of 250 mM adenosine diphosphate, ADP) were added to establish basal OCR. Then, oligomycin A (4 mg/L final concentration, Sigma) was injected into the chamber to inhibit ATP synthase-dependent respiration and induce a proton leak state. OCR measurements at this stage represent only respiration which is not ATP-synthase dependent. To initiate uncoupling of oxygen consumption, FCCP (240 µg/L final concentration, Cayman) or 6PPD-quinone (10 µg/L final concentration) was injected. Any changes in OCR following inhibition of ATP-synthase-dependent respiration represent action due to addition of the known or suspected uncoupling agents. Finally, antimycin A (200 µg/L final concentration, Cayman) was injected into the chamber to disrupt the mitochondrial membrane and inhibit mitochondrial respiration.^{24,25} OCRs of primary gill cells were obtained from the calibrated respirometer readings, normalized to the density of the cell suspension, and expressed as x -fold changes relative to basal respiration in the absence of mitochondria-perturbing agents. Differences in oxygen consumption rates among treatments were evaluated using two-way ANOVA with Holm–Sidak multiple comparisons tests. Experiments with FCCP were performed with preparations from $n = 4$ individual fish, while experiments with 6PPD-quinone were performed with preparations from $n = 3$ individual fish.

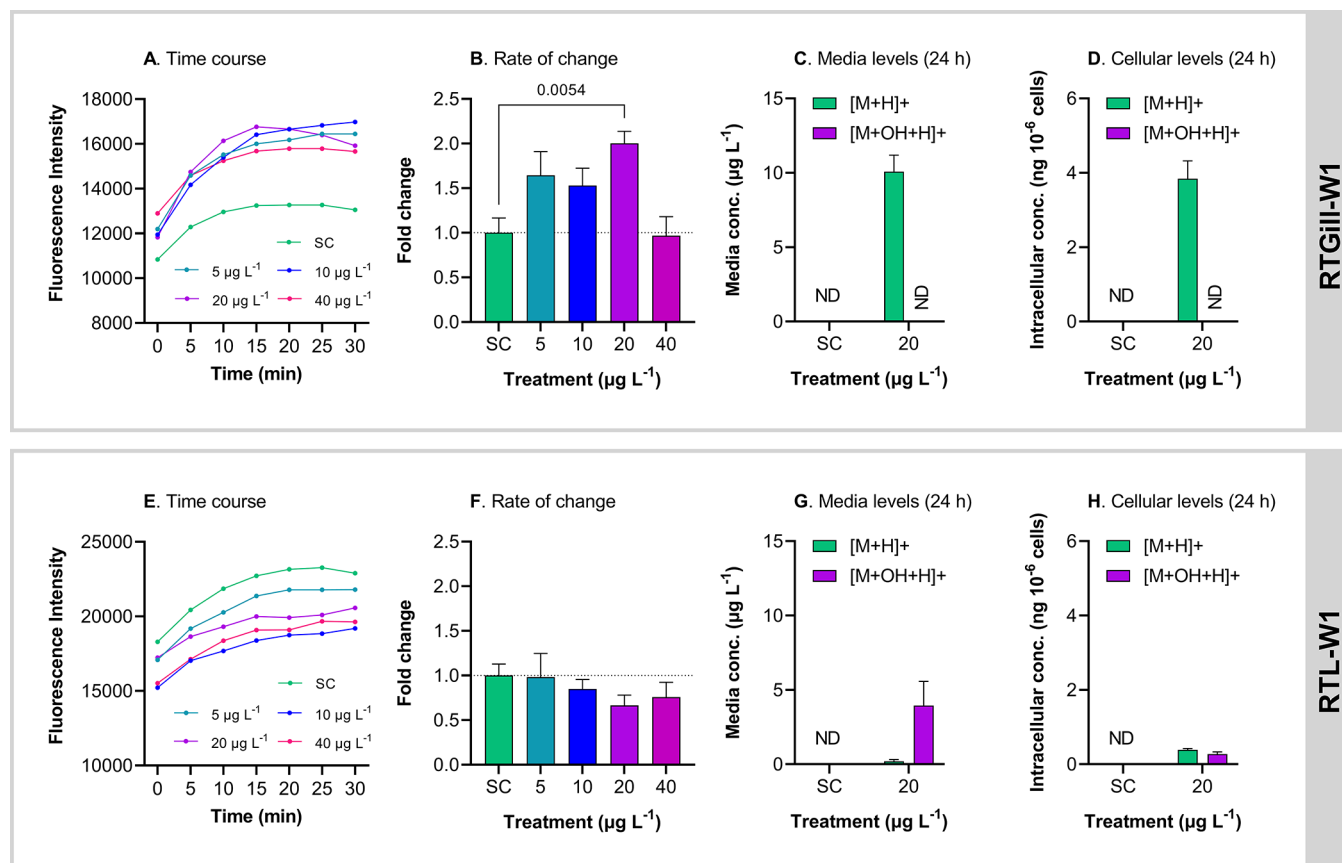


Figure 2. Cellular oxygen consumption rate (OCR), as well as concentrations of 6PPD-quinone and monohydroxylated metabolites in exposure media and RTgill-W1 (top) and RTL-W1 (bottom) cells exposed to graded concentrations of 6PPD-quinone. Time course measurements (A, E) were obtained over a 30 min period (symbols indicate arithmetic means of six technical replicates), and initial rates of change were calculated and expressed as x -fold changes (B,F) relative to those observed in the solvent control ($p \leq 0.05$). Abundances of parent 6PPD-quinone ([M+H]⁺) and a newly discovered monohydroxy metabolite ([M+OH+H]⁺) were determined in culture media (C, G) and cells (D, H) after 24 h exposure to 6PPD-quinone or a solvent control (SC). Bars indicate arithmetic means and error bars the standard deviation of results from triplicate cell culture flasks.

RESULTS AND DISCUSSION

Adherent Cytotoxicity Assay. Exposure of adherent cells to 6PPD-quinone resulted in cell-type specific cytotoxicity (Figure 1). RTgill-W1 cells showed a weak but increasing trend of cell viability up to 40 $\mu\text{g/L}$ followed by a moderate but significant decrease (<20%) at the greatest concentration in both assays (80 $\mu\text{g/L}$; $p \leq 0.05$; Figure 1A and B). This is suggestive of a compensatory response that is overwhelmed at 80 $\mu\text{g/L}$. No cytotoxicity was observed at any concentration of 6PPD-quinone in RTL-W1 cells (Figure 1C and D).

Adherent Cell Oxygen Consumption Rate Assay. At all concentrations of 6PPD-quinone, OCR increased rapidly and then stabilized by 15 min in both cell types (Figure 2A and E). RTgill-W1 cells exposed to 6PPD-quinone at 20 $\mu\text{g/L}$ demonstrated a significant ($p \leq 0.05$) 2.0-fold increase in the rate of increase of OCR relative to the solvent control, whereas there was no increase at other concentrations of 6PPD-quinone (Figure 2B). There were no significant effects of 6PPD-quinone on OCR in RTL-W1 cells (Figure 2F), which suggested that RTgill-W1 cells were more sensitive to 6PPD-quinone than were RTL-W1 cells.

Results with RTgill-W1 cells suggest that 6PPD-quinone might disrupt mitochondrial respiration. This effect might be due to uncoupling of the electron transport chain, caused by dissociation of the mitochondrial membrane potential from

ATP synthesis.²⁶ This effect was only observed in RTgill-W1 cells. Since efficacies of uncouplers are known to differ among species, cell type, and uncoupler used,²⁷ this result suggests that gill cells might be the primary target of toxicity of 6PPD-quinone.

Biotransformation of 6PPD-Quinone. After RTgill-W1 cells were exposed to 20 $\mu\text{g/L}$ 6PPD-quinone for 24 h, 10.1 \pm 1.11 $\mu\text{g/L}$ of 6PPD-quinone was detected in the medium, and 3.84 \pm 0.48 ng/ 10^6 cells were detected in cell extracts (Figure 2C and D). There were no detectable monohydroxy metabolites in either medium or RTgill-W1 cells. Exposure of RTL-W1 cells to 20 $\mu\text{g/L}$ 6PPD-quinone resulted in 0.19 \pm 0.12 $\mu\text{g/L}$ of the parent compound in the medium and 0.39 \pm 0.04 ng/ 10^6 cells in cell extracts (Figure 2G and H). A suspected monohydroxy metabolite (Figure S3) was detected at approximately 3.95 \pm 1.62 $\mu\text{g/L}$ in the medium and 0.27 \pm 0.06 ng/ 10^6 cells in the cell extracts.

These results suggest that 6PPD-quinone was more effectively metabolized by RTL-W1 cells compared to RTgill-W1, for which no monohydroxy metabolite was present. While 6PPD-quinone appears to be available for uptake by RTgill-W1 cells, it did not appear to be effectively biotransformed, allowing for toxicity to be elicited. Thus, differences in cytotoxicity and OCR between RTgill-W1 and RTL-W1 cells could be due to differences in the ability of each cell line to

metabolize 6PPD-quinone. Toxicokinetic drivers of 6PPD-quinone toxicity could be an important future research direction to identify drivers of species-specific sensitivity.

Respirometry Experiments with Suspensions of Primary Gill Cells. Primary rainbow trout gill cells were exposed to subsequent additions of oligomycin A, followed by either FCCP or 6PPD-quinone, followed by antimycin A (Figure 3). Addition of 4 mg/L oligomycin A resulted in a

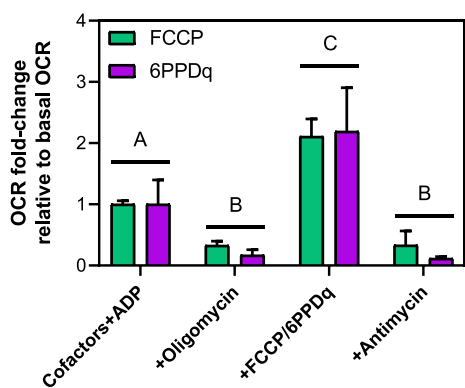


Figure 3. Cellular oxygen consumption rate (OCR) of primary gill cells isolated from subadult rainbow trout with sequential addition of three mitochondria-perturbing agents. Basal OCR measurements were conducted in the presence of cofactors and adenosine diphosphate (ADP) only, with subsequent additions of the adenosine triphosphate (ATP) synthase inhibitor oligomycin A, then either the known uncoupler carbonyl cyanide-*p*-trifluoromethoxyphenylhydrazone (FCCP) or the suspected uncoupler 6PPD-quinone (6PPDq), followed finally by the mitochondrial membrane disruptor antimycin A. Each run consisted of additions of each mitochondria-perturbing agent. OCR measurements were normalized to basal rates in the presence of cofactors and ADP only and expressed as x -fold changes. Bars indicate arithmetic means and error bars the standard deviation of four (FCCP) or three (6PPD-quinone) biological replicates. Different letters indicate significant differences ($p \leq 0.05$) in basal OCR measurements between treatment stages.

significant reduction in OCR ($p \leq 0.05$) by 67.3%–83.2% compared to basal respiration in the presence of only cofactors and ADP. This respiration is equivalent to so-called proton leak respiration.²⁸ Subsequent addition of 240 $\mu\text{g/L}$ FCCP and 10 $\mu\text{g/L}$ 6PPD-quinone resulted in a statistically significant reversion of this leak state ($p \leq 0.05$) and 2.1-fold and 2.2-fold increases in OCR relative to basal respiration, respectively (Figure 3), which is a clear indication of mitochondrial uncoupling.²⁶ Subsequent addition of 200 $\mu\text{g/L}$ antimycin A resulted in a significant reduction in OCR by 66.7%–88.6% compared to basal respiration ($p \leq 0.05$), suggestive of a quantitative disruption of mitochondrial respiration (Figure 3).

CONCLUSION

The current study suggests that acute lethality of salmonids exposed to 6PPD-quinone might be driven by uncoupling of the electron transport chain. This is consistent with the etiology of URMS, including gasping at the surface and increased opercular movement that precede death. Similar effects have been described for the mitochondrial toxicants, including rotenone and FCCP.²⁹ FCCP is a well-characterized and potent mitochondrial uncoupler, and exposure increased OCR in cultured cells³⁰ and embryos.^{17,31} Results of the present study demonstrate that 10 $\mu\text{g/L}$ of 6PPD-quinone had

a similar effect on OCR as 240 $\mu\text{g/L}$ FCCP,^{30,32} supporting the hypothesis that 6PPD-quinone is a potent uncoupler of the electron transport chain. However, this link will need to be established *in vivo* before it can be concluded that mitochondrial uncoupling is the driver of acute lethality resulting from 6PPD-quinone exposure. A previous study *in vivo* by Blair et al. suggested that the acute toxicity could be due to disruption of the blood–brain barrier (BBB);¹¹ however, the conclusions of this study are not necessarily contradictory as further mechanistic studies could provide a link between uncoupling and BBB disruption. Further, considering the conserved nature of the electron transport chain among species³³ and the differences in results obtained with RTgill-W1 and RTL-W1 cells, both in terms of effects on cellular OCR and biotransformation, it appears that sensitivity may at least partly be driven by toxicokinetic factors.

ASSOCIATED CONTENT

Supporting Information

The Supporting Information is available free of charge at <https://pubs.acs.org/doi/10.1021/acs.estlett.2c00431>.

Chromatograms and mass spectra of 6PPD-quinone and the suspected 6PPD-quinone monohydroxy metabolite from various treatments, including negative controls, as well as rainbow trout liver and gill cells (PDF)

AUTHOR INFORMATION

Corresponding Author

Markus Brinkmann – Toxicology Centre, University of Saskatchewan, Saskatoon S7N 5B3, Canada; School of Environment and Sustainability (SENS), University of Saskatchewan, Saskatoon S7N 5CN, Canada; Global Institute for Water Security (GIWS), University of Saskatchewan, Saskatoon S7N 3H5, Canada; orcid.org/0000-0002-4985-263X; Email: markus.brinkmann@usask.ca

Authors

- Hannah Mahoney** – Toxicology Centre, University of Saskatchewan, Saskatoon S7N 5B3, Canada
Francisco C. da Silva Junior – Toxicology Centre, University of Saskatchewan, Saskatoon S7N 5B3, Canada; Department of Cell Biology and Genetics, Biosciences Center, Federal University of Rio, Grande do Norte, Natal, RN 59078-970, Brazil
Catherine Roberts – Toxicology Centre, University of Saskatchewan, Saskatoon S7N 5B3, Canada
Matthew Schultz – Toxicology Centre, University of Saskatchewan, Saskatoon S7N 5B3, Canada
Xiaowen Ji – School of Environment and Sustainability (SENS), University of Saskatchewan, Saskatoon S7N 5CN, Canada
Alper James Alcaraz – Toxicology Centre, University of Saskatchewan, Saskatoon S7N 5B3, Canada; orcid.org/0000-0002-3213-6805
David Montgomery – Toxicology Centre, University of Saskatchewan, Saskatoon S7N 5B3, Canada
Summer Selinger – Toxicology Centre, University of Saskatchewan, Saskatoon S7N 5B3, Canada
Jonathan K. Challis – Toxicology Centre, University of Saskatchewan, Saskatoon S7N 5B3, Canada

John P. Giesy – Toxicology Centre, University of Saskatchewan, Saskatoon S7N 5B3, Canada; Department of Veterinary Biomedical Sciences, Western College of Veterinary Medicine University of Saskatchewan, Saskatoon S7N 5B4, Canada; Department of Environmental Science, Baylor University, Waco, Texas 76706, United States

Lynn Weber – Toxicology Centre, University of Saskatchewan, Saskatoon S7N 5B3, Canada; Department of Veterinary Biomedical Sciences, Western College of Veterinary Medicine University of Saskatchewan, Saskatoon S7N 5B4, Canada

David Janz – Toxicology Centre, University of Saskatchewan, Saskatoon S7N 5B3, Canada; Department of Veterinary Biomedical Sciences, Western College of Veterinary Medicine University of Saskatchewan, Saskatoon S7N 5B4, Canada

Steve Wiseman – Department of Biological Sciences, University of Lethbridge, Lethbridge T1K 3M4, Canada; orcid.org/0000-0002-8215-2272

Markus Hecker – Toxicology Centre, University of Saskatchewan, Saskatoon S7N 5B3, Canada; School of Environment and Sustainability (SENS), University of Saskatchewan, Saskatoon S7N 5CN, Canada

Complete contact information is available at:

<https://pubs.acs.org/10.1021/acs.estlett.2c00431>

Author Contributions

H. Mahoney, F. C. da Silva Junior, and C. Roberts have contributed equally and share first authorship.

Notes

The authors declare no competing financial interest.

ACKNOWLEDGMENTS

This project was supported partially by a financial contribution from Fisheries and Oceans Canada. Additional funding was provided to M.B., L.W., D.J., M.H., J.P.G., and S.W. through the Discovery Grants program of the Natural Sciences and Engineering Research Council of Canada (NSERC). Instrumentation used for chemical analyses within this research was obtained with funding from Western Economic Diversification Canada (WED) and the Canadian Foundation for Innovation (CFI). J.C. was supported through the Banting Postdoctoral Fellowship program of NSERC. H.M. was supported through a Toxicology Centre Devolved Scholarship. F.C.S.J. was supported by Coordination for the Improvement of Higher Education Personnel - CAPES (Process. 88887.570920/2020-00). M.B. is currently a faculty member of the Global Water Futures (GWF) program, which received funds from the Canada First Research Excellence Funds (CFREF). S.W. was supported by a Tier II Canada Research Chair in Aquatic and Mechanistic Toxicology. J.P.G. was supported by the Canada Research Chair Program of NSERC. The authors wish to acknowledge the animal care support of Zoë Henrikson, Azadeh Hatef, and Dale Jefferson (ATRF).

REFERENCES

- (1) Spromberg, J. A.; Scholz, N. L. Estimating the Future Decline of Wild Coho Salmon Populations Resulting from Early Spawner Die-Offs in Urbanizing Watersheds of the Pacific Northwest, USA. *Integrated Environmental Assessment and Management* **2011**, *7* (4), 648–656.
- (2) Walsh, C. J.; Roy, A. H.; Feminella, J. W.; Cottingham, P. D.; Groffman, P. M.; Morgan, R. P. The Urban Stream Syndrome: Current Knowledge and the Search for a Cure. *J. North Am. Benthol Soc.* **2005**, *24* (3), 706–723.

- (3) Chow, M. I.; Lundin, J. I.; Mitchell, C. J.; Davis, J. W.; Young, G.; Scholz, N. L.; McIntyre, J. K. An Urban Stormwater Runoff Mortality Syndrome in Juvenile Coho Salmon. *Aquatic Toxicology* **2019**, *214*, 105231.

- (4) Scholz, N. L.; Myers, M. S.; McCarthy, S. G.; Labenia, J. S.; McIntyre, J. K.; Ylitalo, G. M.; Rhodes, L. D.; Laetz, C. A.; Stehr, C. M.; French, B. L.; McMillan, B.; Wilson, D.; Reed, L.; Lynch, K. D.; Damm, S.; Davis, J. W.; Collier, T. K. Recurrent Die-Offs of Adult Coho Salmon Returning to Spawn in Puget Sound Lowland Urban Streams. *PLoS One* **2011**, *6* (12), e28013.

- (5) Chow, M. I.; Lundin, J. I.; Mitchell, C. J.; Davis, J. W.; Young, G.; Scholz, N. L.; McIntyre, J. K. An Urban Stormwater Runoff Mortality Syndrome in Juvenile Coho Salmon. *Aquatic Toxicology* **2019**, *214*, 105231.

- (6) Tian, Z.; Zhao, H.; Peter, K. T.; Gonzalez, M.; Wetzel, J.; Wu, C.; Hu, X.; Prat, J.; Mudrock, E.; Hettlinger, R.; Cortina, A. E.; Biswas, R. G.; Kock, F. V. C.; Soong, R.; Jenne, A.; Du, B.; Hou, F.; He, H.; Lundeen, R.; Gilbreath, A.; Sutton, R.; Scholz, N. L.; Davis, J. W.; Dodd, M. C.; Simpson, A.; McIntyre, J. K.; Kolodziej, E. P. A Ubiquitous Tire Rubber-Derived Chemical Induces Acute Mortality in Coho Salmon. *Science* **2021**, *371* (6525), 185–189.

- (7) Challis, J. K.; Popick, H.; Prajapati, S.; Harder, P.; Giesy, J. P.; McPhedran, K.; Brinkmann, M. Occurrences of Tire Rubber-Derived Contaminants in Cold-Climate Urban Runoff. *Environmental Science and Technology Letters* **2021**, *8* (11), 961–967.

- (8) Brinkmann, M.; Montgomery, D.; Selinger, S.; Miller, J. G. P.; Stock, E.; Alcaraz, A. J.; Challis, J. K.; Weber, L.; Janz, D.; Hecker, M.; Wiseman, S. Acute Toxicity of the Tire Rubber-Derived Chemical 6PPD-Quinone to Four Fishes of Commercial, Cultural, and Ecological Importance. *Environmental Science and Technology Letters* **2022**, *9* (4), 333–338.

- (9) Hiki, K.; Asahina, K.; Kato, K.; Yamagishi, T.; Omagari, R.; Iwasaki, Y.; Watanabe, H.; Yamamoto, H. Acute Toxicity of a Tire Rubber-Derived Chemical, 6PPD Quinone, to Freshwater Fish and Crustacean Species. *Environ. Sci. Technol. Lett.* **2021**, *8*, 779–784.

- (10) Varshney, S.; Gora, A. H.; Siriypagouder, P.; Kiron, V.; Olsvik, P. A. Toxicological Effects of 6PPD and 6PPD Quinone in Zebrafish Larvae. *Journal of Hazardous Materials* **2022**, *424*, 127623.

- (11) Blair, S. I.; Barlow, C. H.; McIntyre, J. K. Acute Cerebrovascular Effects in Juvenile Coho Salmon Exposed to Roadway Runoff. *Canadian Journal of Fisheries and Aquatic Sciences* **2021**, *78* (2), 103–109.

- (12) Klauschies, T.; Isanta-Navarro, J. The Joint Effects of Salt and 6PPD Contamination on a Freshwater Herbivore. *Sci. Total Environ.* **2022**, *829*, 154675.

- (13) Gerger, C. J.; Weber, L. P. Comparison of the Acute Effects of Benzo-a-Pyrene on Adult Zebrafish (Danio Rerio) Cardiorespiratory Function Following Intraperitoneal Injection versus Aqueous Exposure. *Aquatic Toxicology* **2015**, *165*, 19–30.

- (14) Pasparakis, C.; Mager, E. M.; Stieglitz, J. D.; Benetti, D.; Grosell, M. Effects of Deepwater Horizon Crude Oil Exposure, Temperature and Developmental Stage on Oxygen Consumption of Embryonic and Larval Mahi-Mahi (Coryphaena Hippurus). *Aquatic Toxicology* **2016**, *181*, 113–123.

- (15) Gad, S. C.; Pham, T. Sodium Pentachlorophenate. *Encyclopedia of Toxicology: Third Edition* **2014**, 338–340.

- (16) Salin, K.; Auer, S. K.; Rey, B.; Selman, C.; Metcalfe, N. B. Variation in the Link between Oxygen Consumption and ATP Production, and Its Relevance for Animal Performance. *Proceedings of the Royal Society B: Biological Sciences* **2015**, *282* (1812), na DOI: [10.1098/RSPB.2015.1028](https://doi.org/10.1098/RSPB.2015.1028).

- (17) Souders, C. L.; Liang, X.; Wang, X.; Ector, N.; Zhao, Y. H.; Martyniuk, C. J. High-Throughput Assessment of Oxidative Respiration in Fish Embryos: Advancing Adverse Outcome Pathways for Mitochondrial Dysfunction. *Aquatic Toxicology* **2018**, *199*, 162–173.

- (18) Mosmann, T. Rapid Colorimetric Assay for Cellular Growth and Survival: Application to Proliferation and Cytotoxicity Assays. *Journal of Immunological Methods* **1983**, *65* (1–2), 55–63.

- (19) Repetto, G.; del Peso, A.; Zurita, J. L. Neutral Red Uptake Assay for the Estimation of Cell Viability/Cytotoxicity. *Nature Protocols* **2008**, *3* (7), 1125–1131.
- (20) Brinkmann, M.; Maletz, S.; Krauss, M.; Bluhm, K.; Schiwy, S.; Kuckelkorn, J.; Tiehm, A.; Brack, W.; Hollert, H. Heterocyclic Aromatic Hydrocarbons Show Estrogenic Activity upon Metabolization in a Recombinant Transactivation Assay. *Environ. Sci. Technol.* **2014**, *48* (10), 5892–5901.
- (21) Estabrook, R. W. [7] Mitochondrial Respiratory Control and the Polarographic Measurement of ADP: O Ratios. *Methods Enzymol.* **1967**, *10* (C), 41–47.
- (22) Wood, C. M.; Eletti, B.; Pärt, P. New Methods for the Primary Culture of Gill Epithelia from Freshwater Rainbow Trout. *Fish Physiology and Biochemistry* **2002**, *26* (4), 329–344.
- (23) Gao, M.; Li, A.; Qin, Y.; Liu, B.; Gong, G. Protocol for Measurement of Oxygen Consumption Rate In Situ in Permeabilized Cardiomyocytes. *STAR Protoc* **2020**, *1* (2), 100072.
- (24) Dunshee, B. R.; Leben, C.; Keitt, G. W.; Strong, F. M. The Isolation and Properties of Antimycin A. *J. Am. Chem. Soc.* **1949**, *71* (7), 2436–2437.
- (25) Campo, M. L.; Kinnally, K. W.; Tedeschi, H. The Effect of Antimycin A on Mouse Liver Inner Mitochondrial Membrane Channel Activity. *J. Biol. Chem.* **1992**, *267* (12), 8123–8127.
- (26) Sorgato, M. C.; Lippe, G.; Seren, S.; Ferguson, S. J. Partial Uncoupling, or Inhibition of Electron Transport Rate, Have Equivalent Effects on the Relationship between the Rate of ATP Synthesis and Proton-Motive Force in Submitochondrial Particles. *FEBS Lett.* **1985**, *181* (2), 323–327.
- (27) Demine, S.; Renard, P.; Arnould, T. Mitochondrial Uncoupling: A Key Controller of Biological Processes in Physiology and Diseases. *Cells* **2019**, *8* (8), 795.
- (28) Brand, M. D.; Chien, L. F.; Ainscow, E. K.; Rolfe, D. F. S.; Porter, R. K. The Causes and Functions of Mitochondrial Proton Leak. *Biochim. Biophys. Acta* **1994**, *1187* (2), 132–139.
- (29) Terada, H. Uncouplers of Oxidative Phosphorylation. *Environ. Health Perspect.* **1990**, *87*, 213.
- (30) Plitzko, B.; Loesgen, S. Measurement of Oxygen Consumption Rate (OCR) and Extracellular Acidification Rate (ECAR) in Culture Cells for Assessment of the Energy Metabolism. *BIO-PROTOCOL* **2018**, *8* (10), na DOI: [10.21769/BioProtoc.2850](https://doi.org/10.21769/BioProtoc.2850).
- (31) Stackley, K. D.; Beeson, C. C.; Rahn, J. J.; Chan, S. S. L. Bioenergetic Profiling of Zebrafish Embryonic Development. *PLoS One* **2011**, *6* (9), e25652.
- (32) Cheng, W. W.; Farrell, A. P. Acute and Sublethal Toxicities of Rotenone in Juvenile Rainbow Trout (*Oncorhynchus Mykiss*): Swimming Performance and Oxygen Consumption. *Arch. Environ. Contam. Toxicol.* **2007**, *52* (3), 388–396.
- (33) Vercellino, I.; Sazanov, L. A. The Assembly, Regulation and Function of the Mitochondrial Respiratory Chain. *Nature Reviews Molecular Cell Biology* **2021** 23:2 **2022**, *23* (2), 141–161.

SUPPLEMENTARY INFORMATION

Exposure to the tire rubber-derived contaminant 6PPD-quinone causes mitochondrial dysfunction *in vitro*

Hannah Mahoney & Francisco C. da Silva Junior & Catherine Roberts, Matthew Schultz, Xiaowen Ji, Alper James Alcaraz, David Montgomery, Summer Selinger, Jonathan K. Challis, John P. Giesy, Lynn Weber, David Janz, Steve Wiseman, Markus Hecker, Markus Brinkmann*

Length: Eight pages, five figures.

*Corresponding author: Dr. Markus Brinkmann
School of Environment and Sustainability
University of Saskatchewan
Saskatoon SK, S7N 5C8 Canada
Email: markus.brinkmann@usask.ca



Figure S1: Example chromatograms of negative control RTL-W1 cells for A) parent 6PPD-quinone ($m/z = 299.1760$) and B) suspected mono-hydroxy metabolite ($m/z = 315.1709$) identified using a full-scan MS/dd-MS2 method. Full MS extracted ion chromatograms are filtered with 5 ppm mass tolerance. Negative controls were not exposed to 6PPD-quinone, hence the lack of detection.

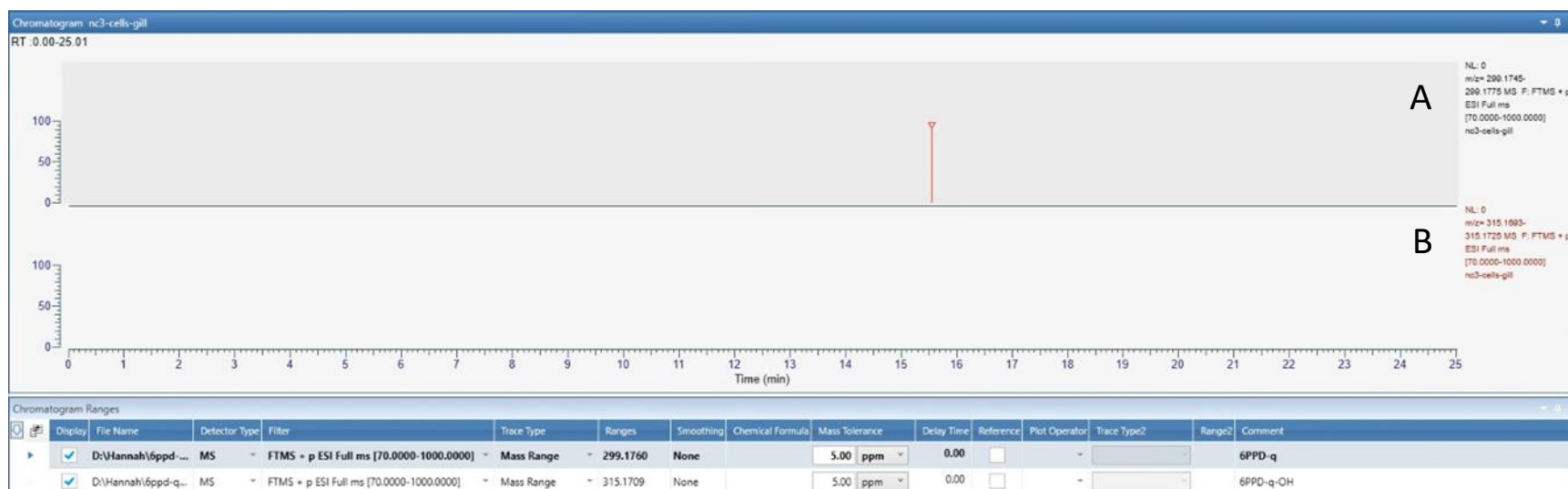
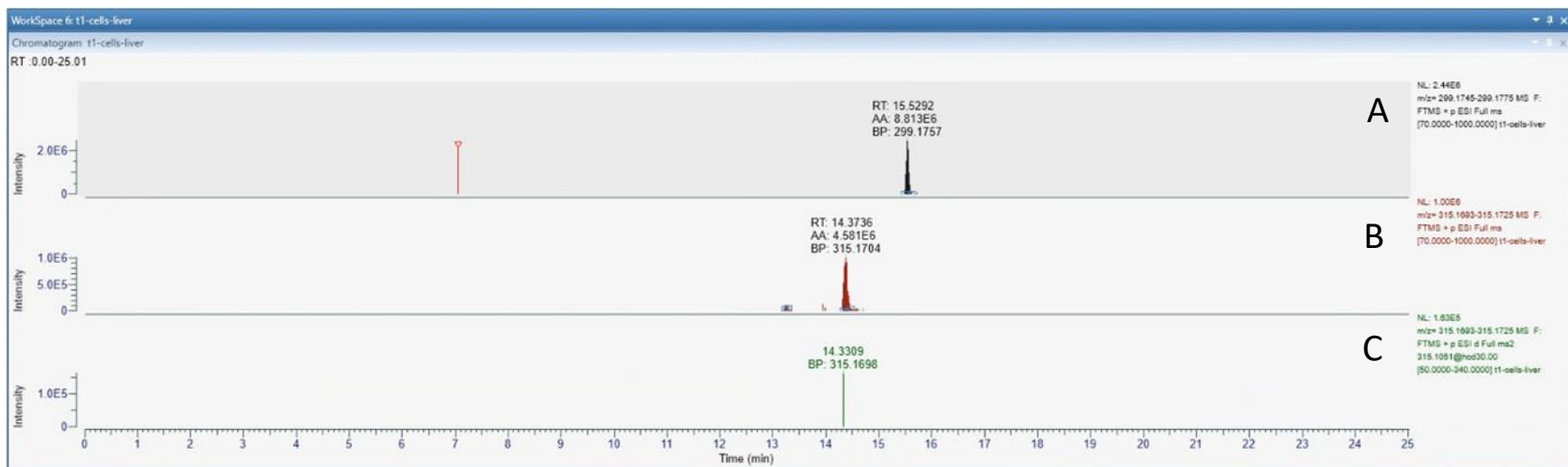
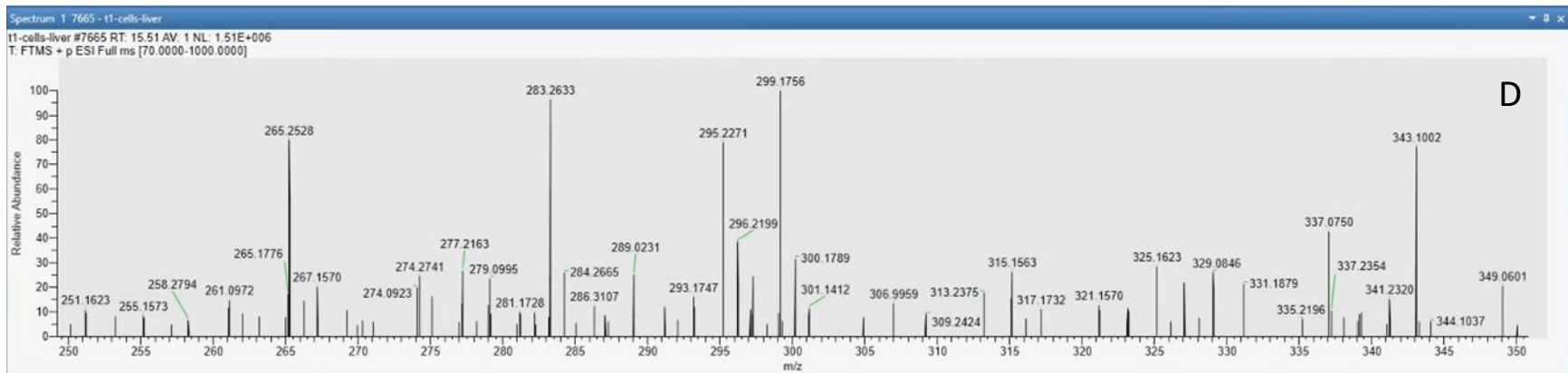


Figure S2: Example chromatograms of negative control RTLgill-W1 cells for A) parent 6PPD-quinone ($m/z = 299.1760$) and B) suspected monohydroxy metabolite ($m/z = 315.1709$) identified using a full-scan MS/dd-MS2 method. Full MS extracted ion chromatograms are filtered with 5 ppm mass tolerance. Negative controls were not exposed to 6PPD-quinone, hence the lack of detection.



Chromatogram Ranges

Display	File Name	Detector Type	Filter	Trace Type	Ranges	Smoothering	Chemical Formula	Mass Tolerance	Delay Time	Reference	Plot Operator	Trace Type?	Range?	Comment
<input checked="" type="checkbox"/>	D:\Hannah\6ppd-...	MS	FTMS + p ESI Full ms [70.0000-1000.0000]	Mass Range	299.1760	None		5.00 ppm	0.00	<input type="checkbox"/>	-	-	-	6PPD-q
<input checked="" type="checkbox"/>	D:\Hannah\6ppd-q...	MS	FTMS + p ESI Full ms [70.0000-1000.0000]	Mass Range	315.1709	None		5.00 ppm	0.00	<input type="checkbox"/>	-	-	-	6PPD-q-OH
<input checked="" type="checkbox"/>	D:\Hannah\6ppd-q...	MS	FTMS + p ESI d Full ms2 315.1051@hcd30.00 [50.0000-340.0000]	Mass Range	315.1709	None		5.00 ppm	0.00	<input type="checkbox"/>	-	-	-	6PPD-q-OH (MS2)



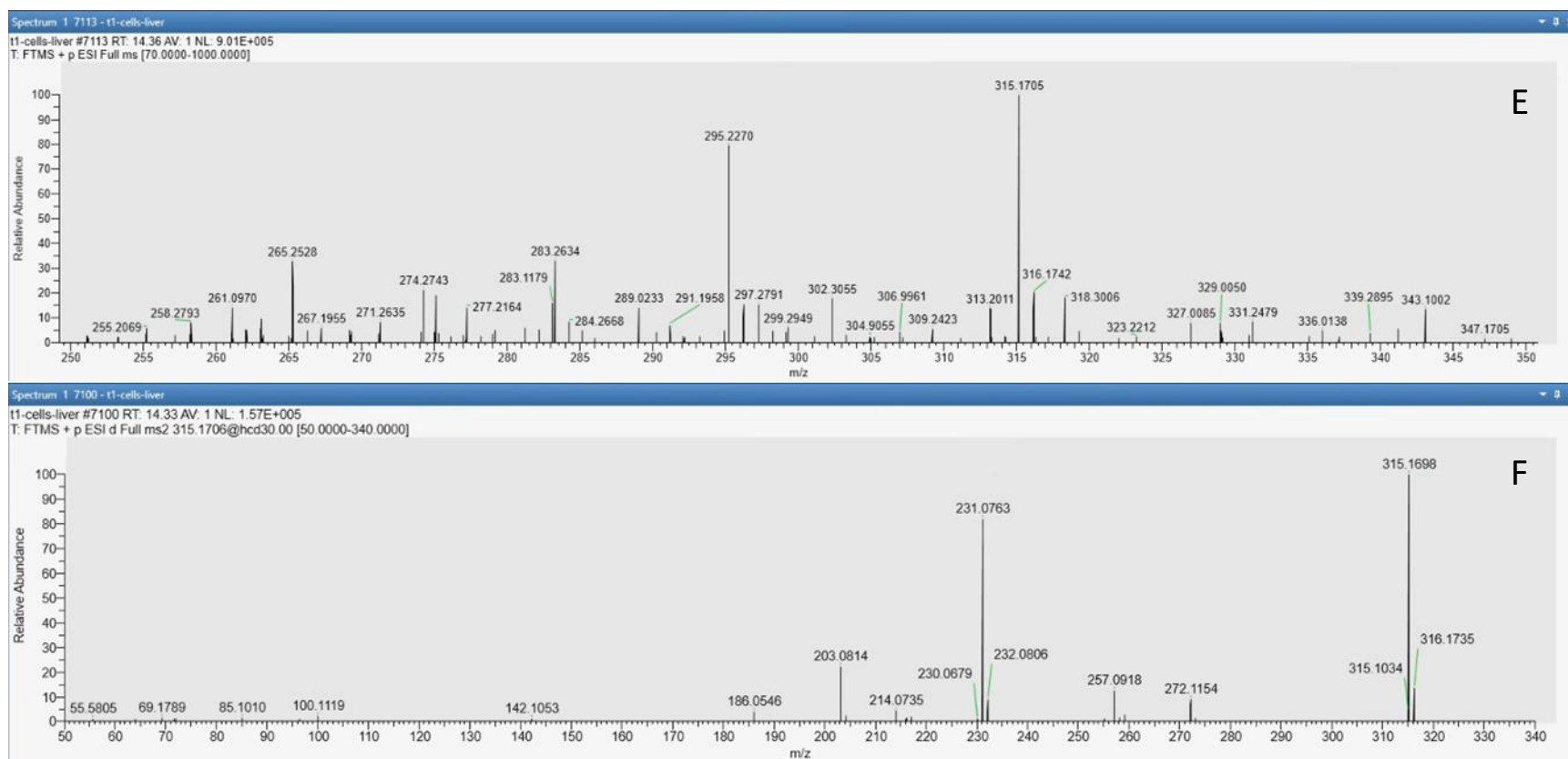
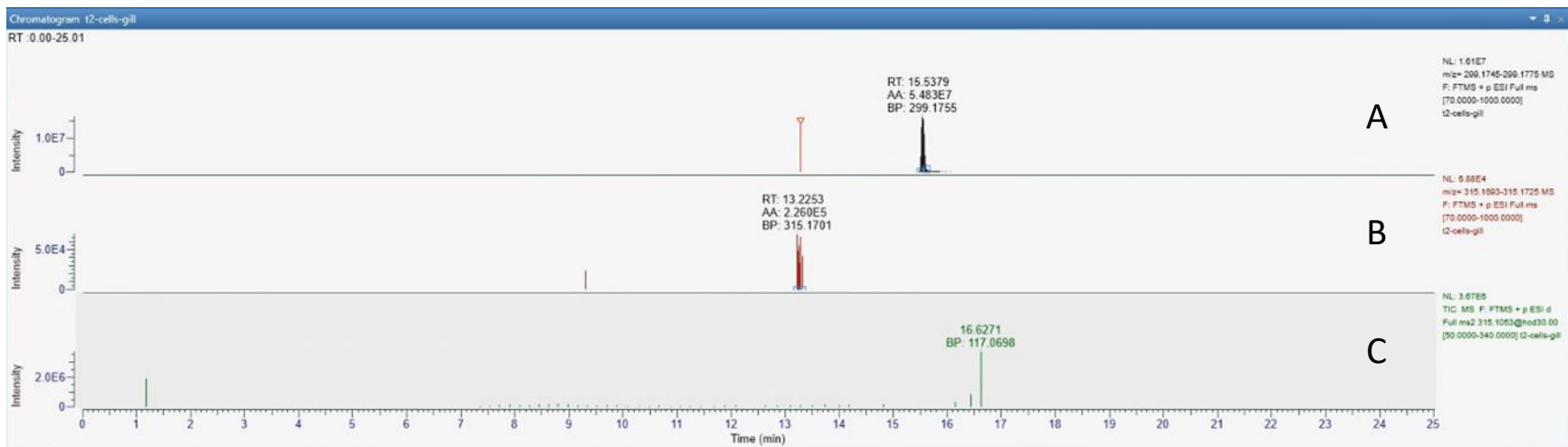
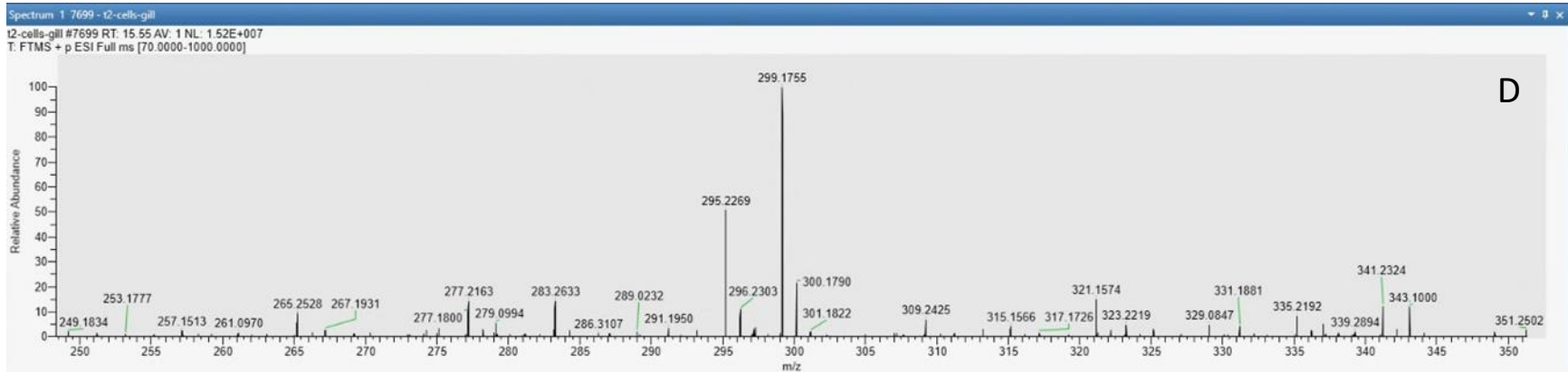


Figure S3: Example chromatograms of exposed RTL-W1 cells for A) full scan parent 6PPD-quinone ($m/z = 299.1760$), B) full scan suspected mono-hydroxy metabolite ($m/z = 315.1709$), and C) the closest selected ddMS2 scan of the suspected mono-hydroxy metabolite ($315.1051 @HCD30$). The corresponding mass spectra of D) 6PPD-quinone full MS (299.1755), E) 6PPD-quinone-OH full MS (315.1705), and F) 6PPD-quinone-OH MS2 ($315.1698 \rightarrow 272.1154, 257.0918, 231.0763, 203.0814$). The MS2 mass spectra of the peak at 14.33 min in C matches the retention of the suspected 6PPD-quinone-OH MS1 peak (315.1704) at 14.37 min in B. The observed fragments of 315.1698 in F are consistent with a 6PPD-quinone mono-hydroxy metabolite as demonstrated in Fig. S5. All extracted ion chromatograms are filtered with 5 ppm mass tolerance.



Chromatogram Ranges

Display	File Name	Detector Type	Filter	Trace Type	Ranges	Smoothing	Chemical Formula	Mass Tolerance	Delay Time	Reference	Plot Operator	Trace Type2	Range2	Comment
<input checked="" type="checkbox"/>	D:\Hannah\6ppd-q...	MS	FTMS + p ESI Full ms [70.0000-1000.0000]	Mass Range	299.1760	None		5.00 ppm	0.00	<input type="checkbox"/>	-			6PPD-q
<input checked="" type="checkbox"/>	D:\Hannah\6ppd-q...	MS	FTMS + p ESI Full ms [70.0000-1000.0000]	Mass Range	315.1709	None		5.00 ppm	0.00	<input type="checkbox"/>	-			6PPD-q-OH
<input checked="" type="checkbox"/>	D:\Hannah\6ppd-...	MS	FTMS + p ESI d Full ms2 315.1053@hcd30.00 [50.0000-340.0000]	TIC		None			0.00	<input type="checkbox"/>	-			6PPD-q-OH (MS2)



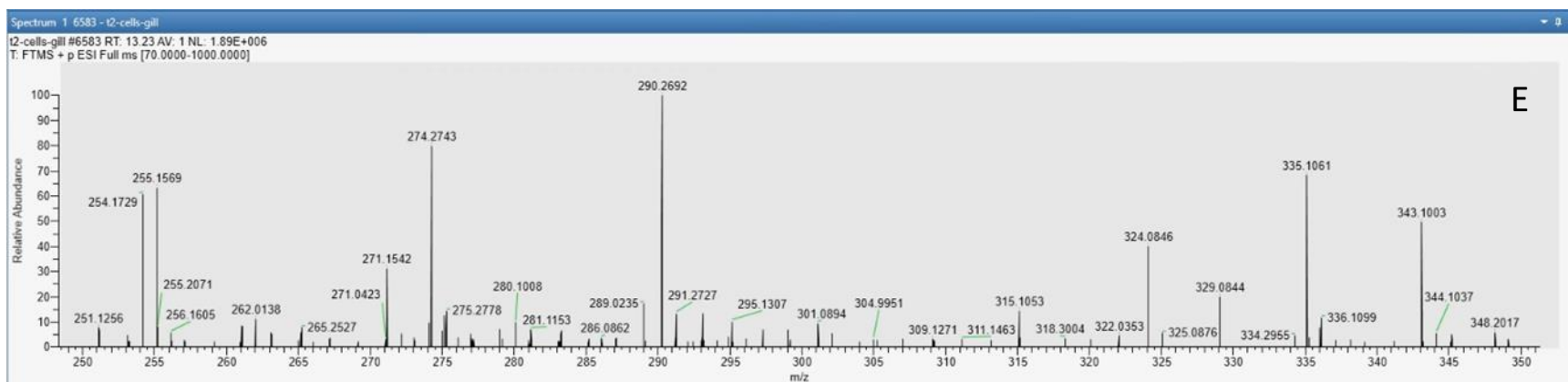


Figure S4: Example chromatograms of exposed RTLgill-W1 cells for A) full scan parent 6PPD-quinone ($m/z = 299.1760$), B) full scan suspected mono-hydroxy metabolite ($m/z = 315.1709$), and C) the closest selected ddMS2 scan of the suspected mono-hydroxy metabolite ($315.1053 @HCD30$). The corresponding mass spectra of D) 6PPD-quinone full MS (299.1755) and E) 6PPD-quinone-OH full MS (expected mass of 315.1709 not present). The MS2 mass spectra at the 13.22 min retention time matching the peak in B is not present and thus not shown. The m/z 315.1701 peak in B is a suspected isobaric interference of the suspected 6PPD-quinone-OH peak of the same m/z (but different retention time) observed in the exposed RTL-W1 cell samples (Fig. S3). The indirect evidence that this is an interference and not the suspected metabolite is three-fold: full MS peak areas in the replicate RTLgill-W1 cell are inconsistent, there is a lack of MS2 data to help elucidate the structure, and the retention time (13.22 min) differs by over 1 min from the 6PPD-quinone-OH peak (14.37 min, Fig. S3) in the RTL-W1 samples (for which MS2 data confirms the proposed mono-hydroxy metabolite structure, Fig. S5). All extracted ion chromatograms are filtered with 5 ppm mass tolerance.



Figure S5: MS2 mass spectra of RTL-W1 cell samples for A) 6PPD-quinone (299.12755 → 256.1204, 241.0971, 215.0815, 187.0865) and B) 6PPD-quinone-OH (315.1698 → 272.1154, 257.0918, 231.0763, 203.0814). The red arrows indicate the major fragments that are consistent with the [M+OH]⁺ fragmentation pattern that the mono-hydroxy metabolite would be expected to produce. The fragmentation in A is consistent with 6PPD-quinone analytical standards here and in our previous research (Challis et al., 2022). None of the MS2 fragments in B were observed for the RTLgill-W1 cell samples.